

First Charm Hadroproduction Results from SELEX[†]

The SELEX Collaboration

J. Russ³, N. Akchurin¹⁷, V. A. Andreev¹¹, A.G. Atamantchouk¹¹, M. Aykac¹⁷, M.Y. Balatz⁸, N.F. Bondar¹¹, A. Bravar²², M. Chensheng⁷, P.S. Cooper⁵, L.J. Dauwe¹⁸, G.V. Davidenko⁸, U. Dersch⁹, A.G. Dolgolenko⁸, D. Dreossi²², G.B. Dzyubenko⁸, R. Edelstein³, A.M.F. Endler⁴, J. Engelfried^{5,13}, C. Escobar^{21,a}, I. Eschrich^{9,b}, A.V. Evdokimov⁸, T. Ferbel¹⁹, I.S. Filimonov^{10,c}, F. Garcia²¹, M. Gaspero²⁰, S. Gerzon¹², I. Giller¹², G. Ginther¹⁹, V.L. Golovtsov¹¹, Y.M. Goncharenko⁶, E. Gottschalk^{3,5}, P. Gouffon²¹, O.A. Grachov^{6,d}, E. Gülmez², C. Hammer¹⁹, M. Iori²⁰, S.Y. Jun³, A.D. Kamenski⁸, H. Kangling⁷, M. Kaya¹⁷, C. Kenney¹⁶, J. Kilmer⁵, V.T. Kim¹¹, L.M. Kochenda¹¹, K. Königsmann^{9,e}, I. Konorov^{9,f}, A.A. Kozhevnikov⁶, A.G. Krivshich¹¹, H. Krüger⁹, M.A. Kubantsev⁸, V.P. Kubarovskiy⁶, A.I. Kulyavtsev^{6,c}, N.P. Kuropatkin¹¹, V.F. Kurshetsov⁶, A. Kushnirenko³, S. Kwan⁵, J. Lach⁵, A. Lamberto²², L.G. Landsberg⁶, I. Larin⁸, E.M. Leikin¹⁰, M. Luksys¹⁴, T. Lungov^{21,g}, D. Magarrel¹⁷, V.P. Maleev¹¹, D. Mao^{3,h}, S. Masciocchi^{9,i}, P. Mathew^{3,j}, M. Mattson³, V. Matveev⁸, E. McCliment¹⁷, S.L. McKenna¹⁵, M.A. Moinester¹², V.V. Molchanov⁶, A. Morelos¹³, V.A. Mukhin⁶, K. Nelson¹⁷, A.V. Nemitkin¹⁰, P.V. Neoustroev¹¹, C. Newsom¹⁷, A.P. Nilov⁸, S.B. Nurushev⁶, A. Ocherashvili¹², G. Oleynik^{5,h}, Y. Onel¹⁷, E. Ozel¹⁷, S. Ozkorucuklu¹⁷, S. Parker¹⁶, S. Patrichev¹¹, A. Penzo²², P. Pogodin¹⁷, B. Povh⁹, M. Procario³, V.A. Prutskoi⁸, E. Ramberg⁵, G.F. Rappazzo²², B. V. Razmyslovich¹¹, V. Rud¹⁰, P. Schiavon²², V.K. Semyatchkin⁸, Z. Shuchen⁷, J. Simon⁹, A.I. Sitnikov⁸, D. Skow⁵, P. Slattery¹⁹, V.J. Smith^{15,k}, M. Srivastava²¹, V. Steiner¹², V. Stepanov¹¹, L. Stutte⁵, M. Svoiski¹¹, N.K. Terentyev^{11,3}, G.P. Thomas¹, L.N. Uvarov¹¹, A.N. Vasiliev⁶, D.V. Vavilov⁶, V.S. Verebryusov⁸, V.A. Victorov⁶, V.E. Vishnyakov⁸, A.A. Vorobyov¹¹, K. Vorwalter^{9,l}, Z. Wenheng⁷, J. You³, L. Yunshan⁷, M. Zhenlin⁷, L. Zhigang⁷, M. Zielinski¹⁹, R. Zukanovich Funchal²¹

¹ Ball State University, Muncie, IN 47306, U.S.A.

² Bogazici University, Bebek 80815 Istanbul, Turkey

³ Carnegie-Mellon University, Pittsburgh, PA 15213, U.S.A.

⁴ Centro Brasileiro de Pesquisas Físicas, Rio de Janeiro, Brazil

⁵ Fermilab, Batavia, IL 60510, U.S.A.

⁶ Institute for High Energy Physics, Protvino, Russia

⁷ Institute of High Energy Physics, Beijing, PR China

⁸ Institute of Theoretical and Experimental Physics, Moscow, Russia

⁹ Max-Planck-Institut für Kernphysik, 69117 Heidelberg, Germany

¹⁰ Moscow State University, Moscow, Russia

¹¹ Petersburg Nuclear Physics Institute, St. Petersburg, Russia

¹² Tel Aviv University, 69978 Ramat Aviv, Israel

¹³ Universidad Autónoma de San Luis Potosí, San Luis Potosí, Mexico

¹⁴ Universidade Federal da Paraíba, Paraíba, Brazil

¹⁵ University of Bristol, Bristol BS8 1TL, United Kingdom

¹⁶ University of Hawaii, Honolulu, HI 96822, U.S.A.

¹⁷ University of Iowa, Iowa City, Iowa 52242, U.S.A.

¹⁸ University of Michigan-Flint, Flint, MI 48502, U.S.A.

¹⁹ University of Rochester, Rochester, NY 14627, U.S.A.

²⁰ University of Rome "La Sapienza" and INFN, Rome, Italy

²¹ University of São Paulo, São Paulo, Brazil

²² University of Trieste and INFN, Trieste, Italy

The SELEX experiment (E781) at Fermilab is a 3-stage magnetic spectrometer for the high statistics study of charm hadroproduction out to large x_F using 600 GeV Σ^- , p and π beams. The main features of the spectrometer are:

- high precision silicon vertex system
- broad-coverage particle identification with TRD and RICH
- 3-stage lead glass photon detector

Preliminary results on differences in hadroproduction characteristics of charm mesons and Λ_c^+ for $x_F \geq 0.3$ are reported. For baryon beams there is a striking asymmetry in the production of baryons compared to antibaryons. Leading particle effects for all incident hadrons are discussed.

1 Introduction

Understanding charm hadroproduction at fixed-target energies has been a difficult theoretical problem because of the complexities of renormalization scale, of parton scale, and of hadronization corrections. The recent review by Frixione, Mangano, Nason, and Ridolfi summarizes the theoretical situation, using data through 1996¹. More recent data from Fermilab E791 (500 GeV π^- beam) greatly improves the statistical precision on charm meson production by pions, but E791 has not yet reported absolute cross sections or compared yields between charm species. In this first report of the SELEX hadroproduction results, we compare our pion results at 580 GeV with those from E791 as well as comparing SELEX pion data with our proton data at 550 GeV and Σ^- data at 620 GeV mean momenta. All SELEX data were taken in the same spectrometer with the same trigger. We limit this report to data having $x_F \geq 0.3$, where the spectrometer acceptance is essentially constant with x_F for all final states.

2 The Experiment

SELEX used the Fermilab Hyperon beam in negative polarity to make a mixed beam of Σ and π in roughly equal numbers. In positive polarity, protons comprised 92% of the particles, with π^+ making up the balance. The beam was run at 0 mrad production. The experiment aimed especially at understanding charm production in the forward hemisphere and was built to have good mass and vertex resolution for charm momenta from 100-500 GeV/c. The spectrometer is shown in Figure 1.

Interactions occurred in a target stack of 5 foils: 2 Cu and 3 C. Total target thickness was 5% of Λ_{int} for protons. Each foil was spaced by 1.5 cm from its neighbors. Decays occurring inside the volume of a target were rejected in this analysis. Interactions were selected by a scintillator trigger. The charm trigger was very loose, requiring only ≥ 4 charged tracks in a forward 10° cone and ≥ 2 hits in a hodoscope after the second analyzing magnet. We triggered on about 1/3 of all inelastic interactions.

A major innovation in E781 was the use of online selection criteria to identify reconstructable events. This experiment uses a RICH counter to identify p , K , or π after the second analyzing magnet. A computational filter used only these RICH-identifiable tracks to make a full vertex reconstruction in the vertex silicon and downstream PWCs. It selected events that had evidence for a secondary vertex. This reduced the data size (and offline computation time) by a factor of nearly 8 at a cost of about a factor of 2 in charm written to tape, as normalized from a study of unfiltered K_s^0 and Λ^0 decays. Most

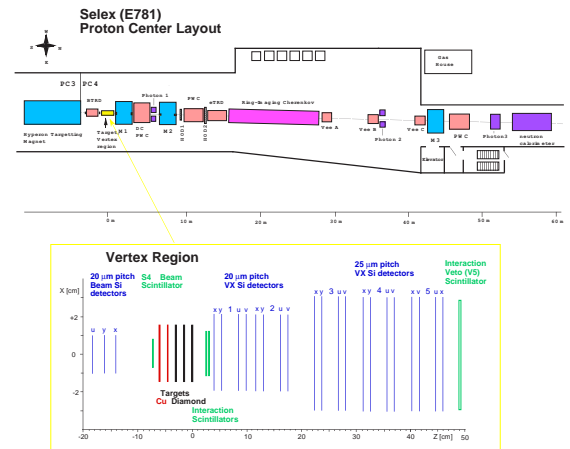


Figure 1: E781 Layout

of the charm loss came from selection cuts that are independent of charm species or kinematic variables. No bias is expected from the filter. Filter operation depends on stable track reconstruction and detector alignment. These features were monitored online and were extremely stable throughout the run.

3 Charm Selection

All data reported here result from a preliminary pass through the data, using a production code optimized for speed but not efficiency. Final yields will be higher than these preliminary results. However, our simulations indicate that the inefficiency does not affect the kinematic features of the results for $x_F \geq 0.3$. For all final states, the charm selection required that the primary vertex lie within the target region and that the secondary vertex occur before the start of the VX silicon. At our high energy, this latter cut removed a number of D^\pm events which can be recovered later.

In this analysis secondary vertices were reconstructed when the vertex χ^2 for the ensemble of tracks was inconsistent with a single primary vertex. All combinations of tracks were investigated, and every secondary vertex candidate was tested against a reconstruction table that listed acceptable particle identification tags for a charm candidate, track selection criteria necessary (RICH identification for a proton, for example), and any other selections, e.g., minimum significance cut for primary/secondary vertex separation. Selected events were written to output files and the essential reconstruction features for each identified secondary vertex were saved in a PAW-like output structure for quick pass-II analysis. All data shown here come from analysis using

this reduced output.

3.1 System performance for charm

Vertex resolution is a critical factor in charm experiments. The primary and secondary longitudinal vertex resolution for all data in a typical run of the experiment are shown in Figure 2. The lower plot shows the primary vertex distribution overlaid on rectangles that represent the physical placement of the 5 targets. The average relativistic transformation factor from lab time to proper time for charm states in these data is 100. This spatial resolution corresponds to about a 20 fs proper time resolution for lifetime studies.

Another important factor in charm studies at large x_F is having good charm mass resolution at all momenta. Figure 3 shows that the measured width of the $D^0 \rightarrow K^- + \pi^+$ is about 10 MeV for all x_F .

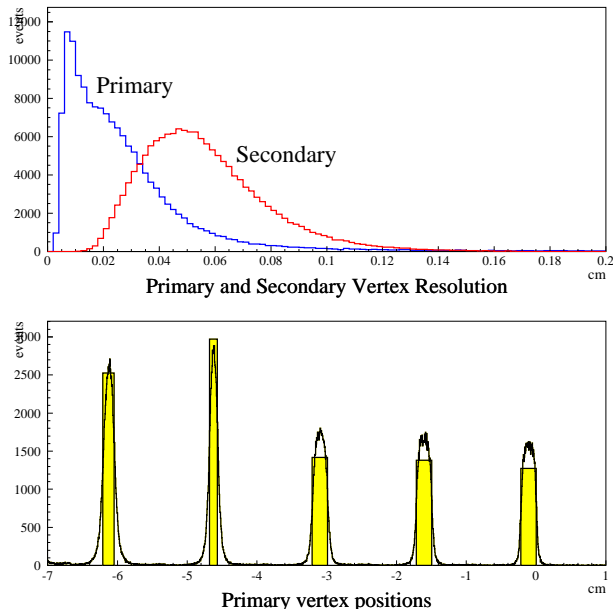


Figure 2: Typical Primary and Secondary Vertex Error Distributions

Finally, we depend on the RICH to give correct identification of K and p decay prongs. Figure 4 shows the π/K separation in interaction data for 100 GeV/c tracks, a typical momentum for prongs from our charm states. The RICH gives π/K separation up to 165 GeV/c (2σ confidence level)².

4 Overall Charm Features at Large x_F

Previous high-statistics charm production results from pions³ and protons⁴ have emphasized central production,

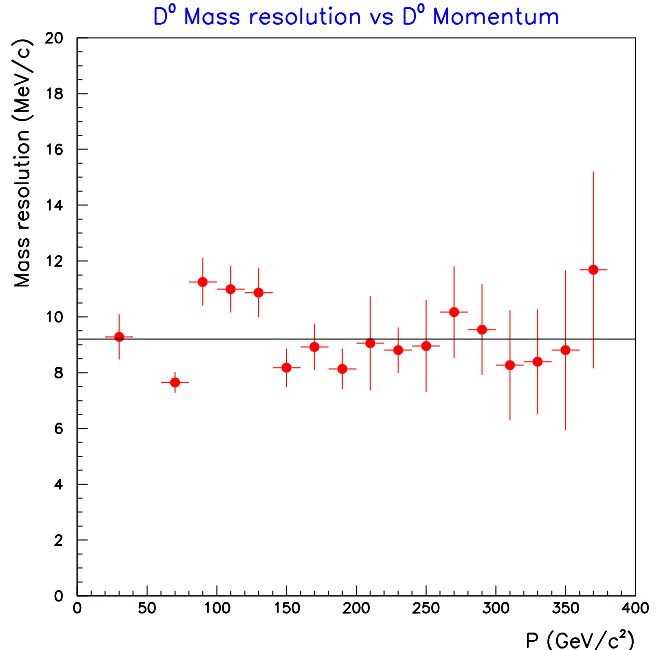


Figure 3: D^0 Mass Resolution versus D^0 Momentum

although both NA32 and E791 have presented results for $x_F \geq 0.5$. SELEX and E769 are the only high energy experiments reporting results from three different beam particles with identical systematics. The important features of the SELEX data can be seen at a glance in Figure 5 for the charged states D^\pm , Λ_c^+ , and $\bar{\Lambda}_c^-$ produced respectively by Σ^- , π^- , and proton beams. The pion data show comparable particle and antiparticle yields both for charm mesons and for charm baryons, as reported by NA32 at lower energy³. It remains a surprising feature of hadroproduction that one finds significant antibaryon production from pions even at $x_F \geq 0.5$. The source of the antiquark pair which combines with the charmed antiquark has been the subject of considerable theoretical speculation. The pion provides a \bar{u} valence quark which can contribute in some models. No present model gives an adequate description. There is good agreement for the D^\pm production asymmetry integrated over $x_F \geq 0.3$ between these preliminary results and the E791 results³. E791 has not published Λ_c^+ asymmetry results. Their observations are consistent with these shown here⁵.

The relative efficiencies for each beam particle are almost the same in this x_F region, so that one can quote the ratio of the cross sections even though we have not yet determined absolute yields. The normalization between different incident hadrons depends on the number of incident beam particles for each data sample and on the total inelastic cross section for each beam particle. We use 34 mb for the proton inelastic cross section, 27

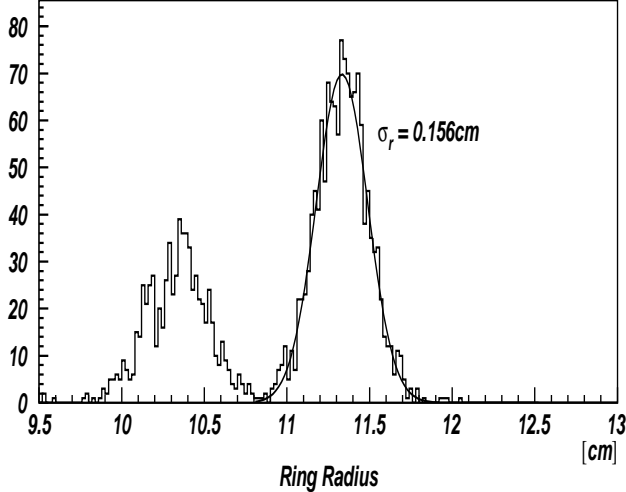


Figure 4: RICH K and π Response at 100 GeV/c

mb for Σ^- , and 22 mb for π^- to compare yields for different beam particles. For these data the relative yields of selected charmed states, normalized to pion production, are given in Table 1. No errors are included in this preliminary analysis. Note that this table does not directly provide information about the relative yields for the different charmed states.

Relative Charmed Particle Yields	p	π^-	Σ^-
$\bar{\Lambda}_c^-$	0.25	1.0	1.1
Λ_c^+	0.9	1.0	1.2
D^-	0.4	1.0	0.8
D^+	0.2	1.0	0.4

Table 1: Relative Charmed Particle Yields for $x_F \geq 0.3$ versus beam type

Perhaps the most surprising result from this table is the observation that baryon beams are very effective charm baryon producers, at least at large x_F . Also, for the states listed here, the Σ^- beam has yields comparable to pions, except for the non-leading case of the D^+ . We have not yet compiled the yields for the c-s-q baryons, where we expect the Σ^- beam relative yields will be large.

The previous table gave the relative efficacy of each beam particle for producing a given charm state at large x_F . It does *not* compare relative yields of the different charm states for the same beam. As can be seen from Figure 5, there are strong asymmetries. These are tabulated in Table 2. Again, errors are omitted at this stage of analysis.

Table 2 shows for both baryon beams there are striking differences in production asymmetries for charm

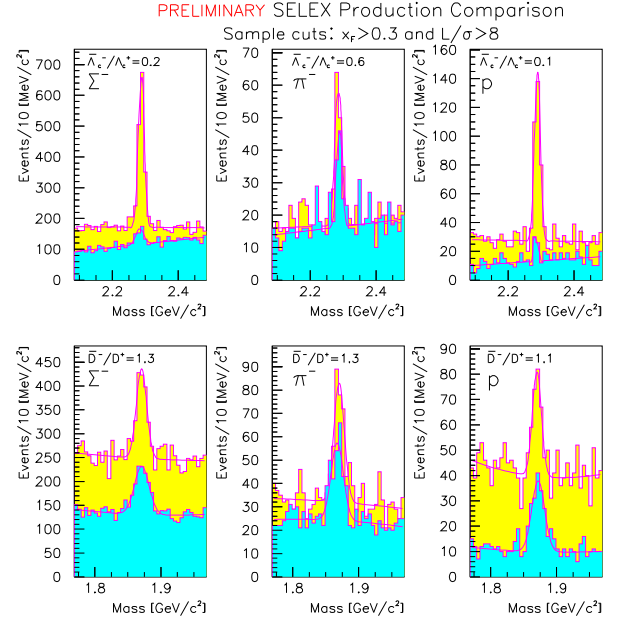


Figure 5: Charm and Anticharm mass distributions for Σ^- , π^- , and p beams in modes $\Lambda_c^- \rightarrow pK^- \pi^+$ or c.c. and $D^+ \rightarrow K^- \pi^+ \pi^+$ or c.c.

Yield Ratio	p	π^-	Σ^-
$\bar{\Lambda}_c^- / \Lambda_c^+$	0.1	0.6	0.2
D^- / D^+	1.1	1.2	1.3

Table 2: Charmed Particle Antiparticle Ratios for $x_F \geq 0.3$ versus beam type

baryons compared to the pion beam. For charm mesons, that is not the case. Baryon beams, which have no valence antiquarks, show strong suppression of antibaryon production, compared to pions. This feature was not observed by NA27 in 400 GeV pp collisions. They reported comparable baryon/antibaryon production but had only a few events, all in the central region. No other proton data exist for charm baryons. The WA99 results for charm baryon production by Σ^- are consistent with our findings⁶.

The D^- and Λ_c^+ are leading hadrons in the sense that all 3 beam hadrons *may* contribute at least one valence quark to the final state. The large difference in the Λ_c^+ asymmetry between the meson beam (largely symmetric) and the baryon beams (very asymmetric) is a new issue for charm hadroproduction analysis, which has assumed that there is a universal baryon/meson fraction for all incident hadrons¹.

5 Summary

The SELEX experiment complements previous charm hadroproduction experiments by exploring different regions of production phase space and by using different beams. The early results already show some noteworthy new features of charm production. Further studies of different states and details of single- and double-differential charm production distributions are underway and will be reported at meetings in the fall.

Further analysis will extend the x_F coverage down to about 0.1, to enhance overlap with other experiments and to increase statistics. Also, other charm baryon states are being analyzed and results will be reported later.

Acknowledgements

We are indebted to the technical staff at Fermilab and our home institutions, especially B. C. LaVoy, D. Northacker, F. Pearsall, and J. Zimmer, for invaluable technical support. This project was supported in part by Bundesministerium für Bildung, Wissenschaft, Forschung und Technologie, Consejo Nacional de Ciencia y Tecnología (CONACyT), Conselho Nacional de Desenvolvimento Científico e Tecnológico, Fondo de Apoyo a la Investigación (UASLP), Fundação de Amparo à Pesquisa do Estado de São Paulo (FAPESP), the Israel Science Foundation founded by the Israel Academy of Sciences and Humanities, Istituto Nazionale de Fisica Nucleare (INFN), the International Science Foundation (ISF), the National Science Foundation, NATO, the Russian Academy of Science, the Russian Ministry of Science and Technology, the Turkish Scientific and Technological Research Board (TÜBİTAK), the U.S. Department of Energy, and the U.S.-Israel Binational Science Foundation (BSF).

References

1. S. Frixione, M. Mangano, P. Nason, and G. Ridolfi, “Heavy Quark Production” in “Heavy Flavours II”, A. J. Buras and M. Lindner, eds., World Scientific Publishing Co, Singapore (1997); see also preprint hep-ph/9702287
2. Fermilab-Pub-98/299-E, submitted to Nucl. Instr. & Methods.
3. NA32: 230 GeV; S. Barlag, et al., Z. Phys. **C39** (1988) 451; *ibid* **C49** (1991) 555; Phys. Lett. **B257** (1991) 519
E769: 250 GeV; G.A. Alves, et al., Phys. Rev. Lett. **69** (1992) 3147; *ibid* **77** (1996) 2388; 2392
WA92: 330 GeV; M.I. Adamovich, Phys. Lett. **B348** (1995) 256; *ibid* **B385** (1996) 487; Nucl. Phys. **B495** (1997) 3
E791: 500 GeV; E.M. Aitala, et al., Phys. Lett. **B411** (1997) 230; *ibid* **B403** (1997) 185; *ibid* **B371** (1996) 157
4. E769: 250 GeV; G.A. Alves, et al., Phys. Rev. Lett. **77** (1996) 2388; 2392
NA27: 400 GeV; M. Aguilar-Benitez, et al., Z. Phys. **C40** (1988) 321
5. Simon Kwan, private communication
6. M.I. Adamovich, et al., submitted to Eur. Phys. J. C; preprint hep-ex/9803021

[†]Invited talk presented at the 1998 International Conference on High Energy Physics, Vancouver, B.C., Canada, July, 1998.

^aPresent address: Instituto de Física da Universidade Estadual de Campinas, UNICAMP, SP, Brazil.

^bNow at Imperial College, London SW7 2BZ, U.K.

^cdeceased

^dPresent address: Dept. of Physics, Wayne State University, Detroit, MI 48201, U.S.A.

^ePresent address: Universität Freiburg, 79104 Freiburg, Germany

^fPresent address: Physik-Department, Technische Universität München, 85748 Garching, Germany

^gCurrent Address: Instituto de Física Teórica da Universidade Estadual Paulista, São Paulo, Brazil

^hPresent address: Lucent Technologies, Naperville, IL

ⁱNow at Max-Planck-Institut für Physik, München, Germany

^jPresent address: Motorola Inc., Schaumburg, IL

^kGenerous support of Carnegie-Mellon University is gratefully acknowledged.

^lPresent address: Deutsche Bank AG, 65760 Eschborn, Germany